*Journal of Sound and Vibration* (2001) **245**(5), 953–959
doi:10.1006/jsvi.2000.3566, available online at http://www.idealibrary.com on IDEAL®

# ACOUSTIC BEHAVIOR OF SHORT ELLIPTICAL CHAMBERS WITH END CENTRAL INLET AND END OFFSET OR SIDE OUTLET

A. SELAMET

*Department of Mechanical Engineering and The Center for Automotive Research, The Ohio State University, Columbus, OH* 43210-1107, *U.S.A. E-mail: selamet.1@osu.edu*

AND

F. D. DENIA

*Departamento de Ingeniería Mecánica y de Materiales, Universidad Politécnica de Valencia, Camino de Vera s/n*, 46022 *Valencia, Spain*

(*Received* 1 *December* 2000)

## 1. INTRODUCTION

The elliptical chamber is a commonly used silencer configuration in the breathing system of engines. Yet, with the exception of a few recent investigations, its acoustic behavior has not been studied in detail. Denia *et al.* [1] apply the finite element method (FEM) and the point source technique to analyze such configurations. They provide comparisons with the circular case and some experimental results, establishing that the eccentricity has an important effect on the acoustic performance. In an attempt to represent the production exhaust and tail pipe locations that are usually on the major axis of an ellipse, the authors have considered only the cases with end offset inlet/outlet. The side inlet and outlet ports, on the other hand, are known to modify the acoustic behavior drastically for circular configurations [2, 3]. Therefore, the present study investigates the effect of side ports in elliptical configurations, including the angular locations over the outer surface. The effect of the location of end outlet ports (minor versus major axis) is also examined. The investigation is confined to short chambers, where the transverse propagation dominates [4, 5]. The experimental transmission loss for one selected configuration is shown to agree well with the FEM predictions.

## 2. GEOMETRY AND MODES

Figures 1(a) and (b) show the end central inlet/end offset outlet chamber configurations, with the outlet located on the major and minor axes of the ellipse respectively. Figures 2(a) and (b) depict the end central inlet/side outlet cases with the outlet located on the major axis and the minor axis respectively. For all the cases considered, the inlet and outlet ducts have the same diameter, $d_1 = d_2 = 0{\cdot}04859$ m, the major axis is $2a = 0{\cdot}25$ m and the minor axis is $2b = 0{\cdot}15$ m. Two relatively short chamber lengths $L = 0{\cdot}1$ and $0{\cdot}05$ m are considered primarily to examine the transverse propagation.

Leading to the discussion in the next section, the cut-off frequencies of the higher order modes in the frequency range of interest have been evaluated here. The rigid wall boundary

0022-460X/01/350953 + 07 $35.00/0 © 2001 Academic Press

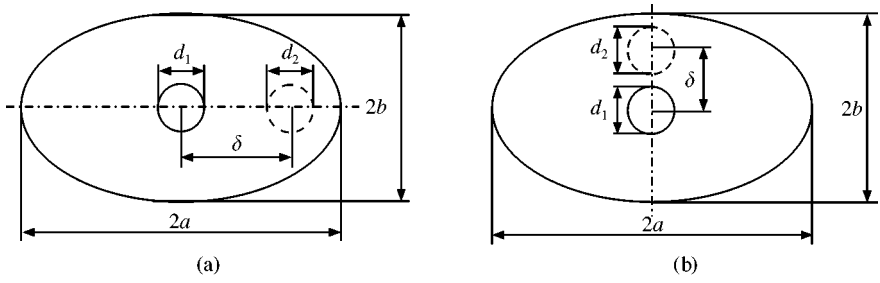


Figure 1. Elliptical chamber with end central inlet/end offset outlet. (a) Outlet on the major axis; (b) outlet on the minor axis.

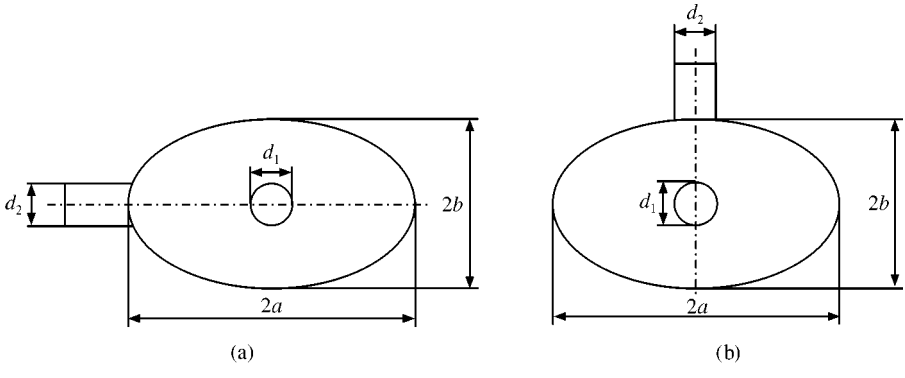


Figure 2. Elliptical chamber with end central inlet/side outlet. (a) Outlet on the major axis; (b) outlet on the minor axis.

condition yields [6]

$$\left.\frac{\partial \mathrm{Ce}_r(u, q)}{\partial u}\right|_{u=u_w} = 0, \quad r = 0, 1, 2, \ldots, \qquad \left.\frac{\partial \mathrm{Se}_r(u, \bar{q})}{\partial u}\right|_{u=u_w} = 0, \quad r = 1, 2, \ldots, \tag{1, 2}$$

where $\mathrm{Ce}_r$ and $\mathrm{Se}_r$ are, respectively, the modified even and odd Mathieu functions of the first kind and order $r$, $u$ is the radial (elliptical) co-ordinate and $u_w$ is its value at the chamber outer wall. Once the roots $q_{r,i}$ and $\bar{q}_{r,i}$, $i = 1, 2, \ldots$, of equations (1) and (2) are evaluated, the associated frequencies can be readily obtained from

$$f_{r,i} = \frac{c_0}{2\pi}\sqrt{\frac{4q_{r,i}}{\rho^2}}, \qquad \bar{f}_{r,i} = \frac{c_0}{2\pi}\sqrt{\frac{4\bar{q}_{r,i}}{\rho^2}}, \tag{3, 4}$$

where $c_0$ is the speed of sound and $\rho$ the semi-interfocal distance. Table 1 gives the first few roots of equations (1) and (2) and the corresponding frequencies for $2a = 0{\cdot}25$ m and $2b = 0{\cdot}15$ m (eccentricity $\varepsilon = \sqrt{1 - b^2/a^2} = 0{\cdot}8$ and semi-interfocal distance $\rho = \varepsilon a = 0{\cdot}1$ m).

Figure 3 depicts the mode shapes associated with the natural frequencies listed in Table 1. As indicated in reference [6], even modes (whose corresponding roots and frequencies are denoted without bar) of even $r$ are symmetric about both axes and even modes of odd $r$ are only symmetric about the major axis. For the odd modes (whose associated values are

TABLE 1
*Roots and frequencies of the higher order modes*

| Order | Root | Frequency (Hz) |
|---|---|---|
| $(r, i)$ | $q_{r,i}$ | $f_{r,i}$ |
| Even modes | | |
| (1, 1) | 0·5584 | 808·76 |
| (2, 1) | 1·8345 | 1465·87 |
| (3, 1) | 3·7714 | 2101·75 |
| (0, 2) | 5·2304 | 2475·12 |
| $(r, i)$ | $\bar{q}_{r,i}$ | $\bar{f}_{r,i}$ |
| Odd modes | | |
| (1, 1) | 1·4247 | 1291·80 |
| (2, 1) | 2·6983 | 1777·76 |
| (3, 1) | 4·5237 | 2301·85 |

denoted with bar), those of odd $r$ are symmetric about the minor axis, and those of even $r$ are not symmetric with respect to any axis.

## 3. RESULTS AND DISCUSSION

The acoustic behavior of different chambers is examined in terms of transmission loss. The chambers with length $L = 0{\cdot}1$ m are studied first, with end offset outlet and side outlet on the axes of the ellipse. The same analysis is then repeated after halving the chamber length ($L = 0{\cdot}05$ m).

Figure 4 shows the results for two end offset outlets ($\delta = 0{\cdot}08$ and $0{\cdot}0515$ m) and a side outlet (located at $L/2$) on the major axis. These three geometries are symmetric about this axis, so only the modes that share the same symmetry may propagate. Figure 3 illustrates that the even modes satisfy this condition, and their corresponding cut-off frequencies are included in Figure 4. For clarity, even and odd modes will hereafter be designated by subscripts "$e$" and "$o$" respectively. The offset value $\delta = 0{\cdot}0515$ m is chosen such that the outlet is located on the nodal line of the $(2, 1)_e$ mode [1]. A concentric chamber is also included for comparison purposes. For the chambers with end offset outlet, $\delta = 0{\cdot}08$ m, and side outlet, the transmission loss is nearly identical until the propagation of the $(2, 1)_e$ mode resulting in a well-defined dome behavior associated with the diametral propagation [7] along the major axis. The peak corresponding to the $(1, 1)_e$ mode has a minor effect, primarily due to the central inlet. Above the cut-off frequency of the $(2, 1)_e$ mode, however, the behavior of these two chambers becomes different, with the side outlet exhibiting a broadband attenuation which may be linked to the outlet location at $L/2$, where the pressure values are low. Thus, the attenuation is improved by the side outlet chamber at higher frequencies. In contrast, the TL collapse of the end offset outlet chamber with $\delta = 0{\cdot}08$ m is evident, with no domes appearing above 1500 Hz. When the outlet is located on the nodal line of the $(2, 1)_e$ mode, the effect of this mode becomes nearly negligible, leading to a wider dome followed by another broad attenuation region before the onset of the $(0, 2)_e$ mode. The behavior of the concentric chamber is rather different above the $(1, 1)_e$ mode with the shorter distance between the inlet and outlet promoting a transverse

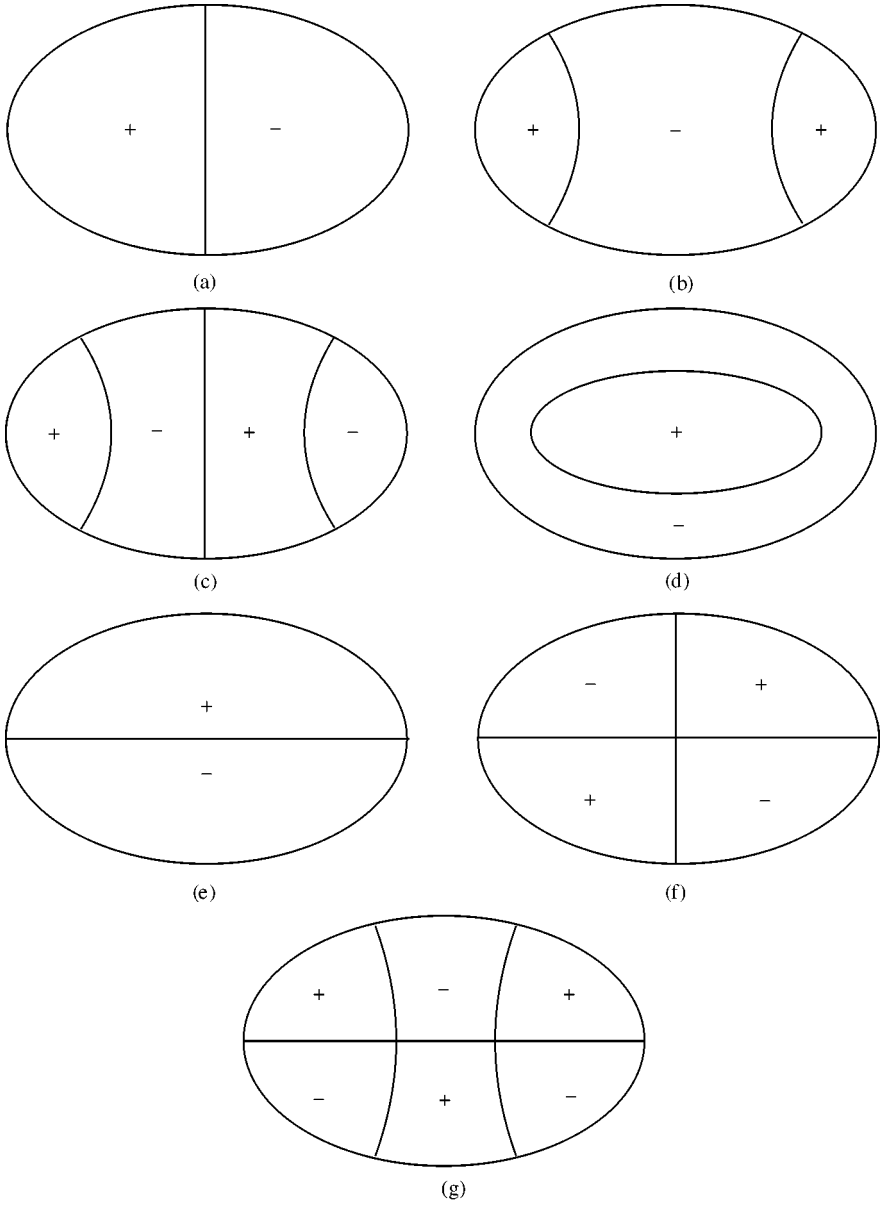


Figure 3. Pressure contours for the elliptical higher order modes: (a) even mode (1, 1); (b) even mode (2, 1); (c) even mode (3, 1); (d) even mode (0, 2); (e) odd mode (1, 1); (f) odd mode (2, 1); (g) odd mode (3, 1).

resonance that eliminates the dome(s). The peak of the $(1, 1)_e$ mode is no longer present, since the symmetry of this chamber does not allow its propagation.

Figure 5 shows the results obtained for the end offset outlet with $\delta = 0{\cdot}04$ m and the side outlet located halfway along the length ($L/2$), with both outlets on the minor axis of the ellipse. The concentric case in Figure 4 is also included for comparison. The first two are now symmetric about the minor axis, so only the cut-off frequencies of the modes that share the same symmetry (even modes of even $r$ and odd modes of odd $r$) are depicted in Figure 5. The elliptical chambers exhibit a different behavior in comparison with those of Figure 4, as

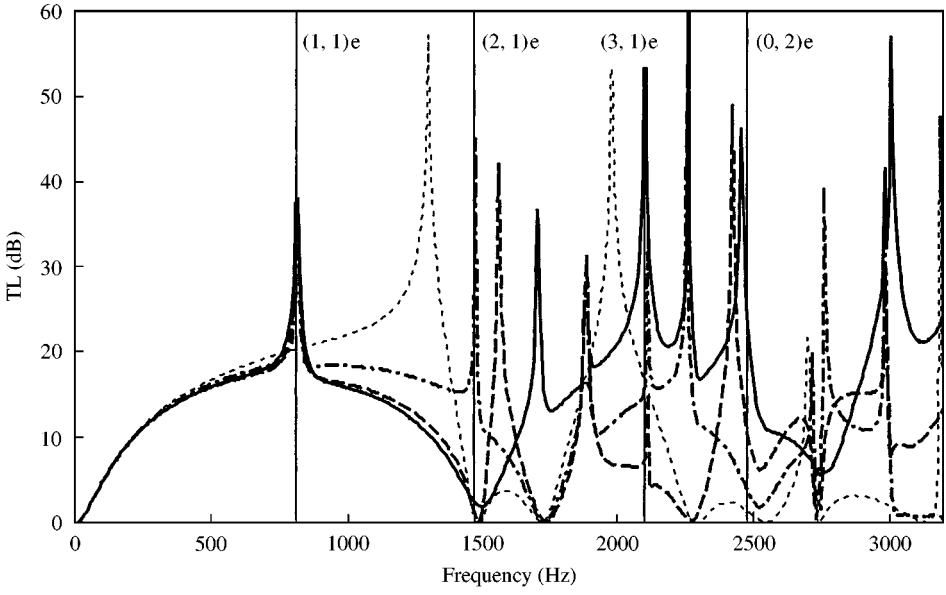


Figure 4. Transmission loss for an elliptical chamber with end offset or side outlets on the major axis with $2a = 0{\cdot}25$ m, $2b = 0{\cdot}15$ m, $d_1 = d_2 = 0{\cdot}04859$ m and $L = 0{\cdot}1$ m: ----, $\delta = 0{\cdot}08$ m; ——, side outlet; -·-·-, $\delta = 0{\cdot}0515$ m; ·····, concentric.

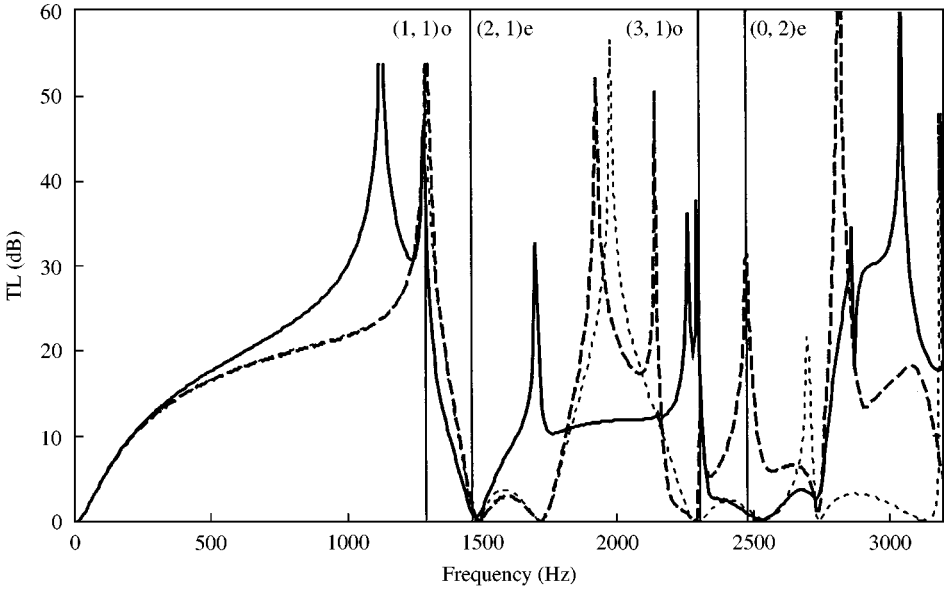


Figure 5. Transmission loss for an elliptical chamber with end offset or side outlets on the minor axis with $2a = 0{\cdot}25$ m, $2b = 0{\cdot}15$ m, $d_1 = d_2 = 0{\cdot}04859$ m and $L = 0{\cdot}1$ m: ----, $\delta = 0{\cdot}04$ m; ——, side outlet; ·····, concentric.

expected, since the shorter distance between the inlet and outlet now leads to a resonance, and the dome associated with the diametral propagation is not present. The end offset and side outlet configurations are now less similar, suggesting that the resonance characteristics are affected by the locations. Below the onset of higher order modes, the attenuation of the

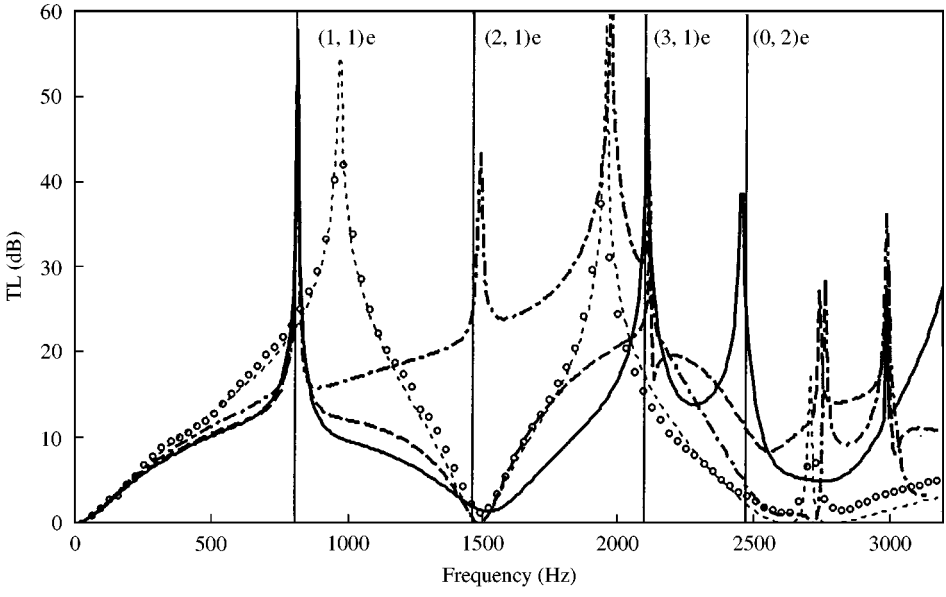


Figure 6. Transmission loss for an elliptical chamber with end offset or side outlets on the major axis with $2a = 0{\cdot}25$ m, $2b = 0{\cdot}15$ m, $d_1 = d_2 = 0{\cdot}04859$ m and $L = 0{\cdot}05$ m: ----, $\delta = 0{\cdot}08$ m; ——, side outlet; -·-·-, $\delta = 0{\cdot}0515$ m; ·····, concentric; ○, experimental concentric.

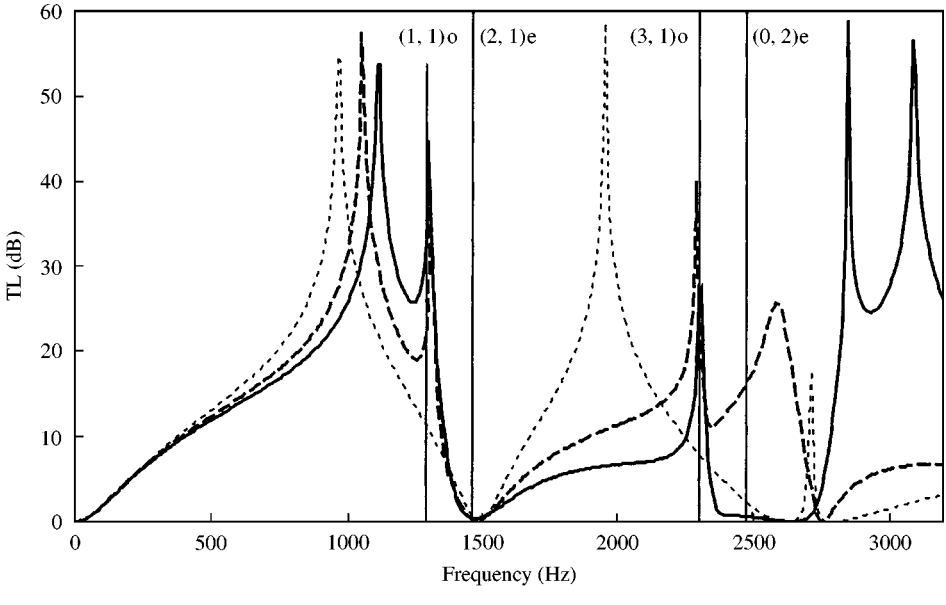


Figure 7. Transmission loss for an elliptical chamber with end offset or side outlets on the minor axis with $2a = 0{\cdot}25$ m, $2b = 0{\cdot}15$ m, $d_1 = d_2 = 0{\cdot}04859$ m and $L = 0{\cdot}05$ m: ----, $\delta = 0{\cdot}04$ m; ——, side outlet; ·····, concentric.

end offset outlet and the concentric chambers is nearly identical, primarily due to the fact that outlets are now closer. There is a transition from dome behavior to resonant behavior as the outlet moves from the major to the minor axis. In the former case (Figure 4), both end offset ($\delta = 0{\cdot}08$ m) and side outlets are rather similar until three-dimensional

propagation dominates. In the latter (Figure 5), more discrepancies are present at lower frequencies.

Figure 6 shows the results for a shortened chamber length $L = 0{\cdot}05$ m with the outlet located on the major axis. The concentric configuration is again included for comparison. The behavior of the side outlet and the end offset outlet with $\delta = 0{\cdot}08$ m is similar below the $(2, 1)_e$ mode, with some deviations observed between the $(1, 1)_e$ and $(2, 1)_e$ modes. Above the $(2, 1)_e$ mode, the two configurations exhibit more similarity in comparison with Figure 4. A near-dome behavior is observed in the attenuation with an amplitude of about 8 dB lower than that in Figure 4, since the cross-sectional area for the diametral propagation is now smaller. When the outlet is located at the nodal line of the $(2, 1)_e$ mode, the acoustic attenuation shows a general improvement. The behavior of this configuration with $\delta = 0{\cdot}0515$ m is different from that of the same chamber with $L = 0{\cdot}1$ m, since a resonance is now observed due to the shorter length. For the concentric case, the short distance between the inlet and outlet also leads to an acoustic resonant response with less similarity at low frequencies in comparison with the end offset and side outlet geometries. The concentric configuration has also been fabricated and its transmission loss has been measured in an extended impedance tube facility described elsewhere [8]. The comparison with the predictions shows a good agreement, as expected.

Moving the outlet to the minor axis changes the acoustic behavior observed in Figure 6 considerably as illustrated in Figure 7. The closer locations of the inlet and outlet result in resonances, with the behavior of the end offset and side outlet configurations now becoming more similar than in Figure 5 at low frequencies.

The acoustic behavior of short elliptical chambers with the end offset and side outlets is found to be similar at low frequencies when the outlet is located on the major axis and for large offset distances. In this configuration, a diametral wave propagation is formed resulting in a broadband dome attenuation. Moving the outlet to the minor axis reduces the distance between inlet and outlet, thereby leading to resonances and increasing the difference between the end and side outlets.

## REFERENCES


1. F. D. Denia, J. Albelda, F. J. Fuenmayor and A. J. Torregrosa 2000 *Journal of Sound and Vibration* **241**, 401–421. Acoustic behaviour of elliptical chamber mufflers.
2. S. I. Yi and B. H. Lee 1986 *Journal of the Acoustical Society of America* **79**, 1299–1306. Three-dimensional acoustic analysis of circular expansion chambers with a side inlet and a side outlet.
3. S. I. Yi and B. H. Lee 1987 *Journal of the Acoustical Society of America* **81**, 1279–1287. Three-dimensional acoustic analysis of a circular expansion chamber with side inlet and end outlet.
4. A. Selamet and P. M. Radavich 1997 *Journal of Sound and Vibration* **201**, 407–426. The effect of length on the acoustic attenuation performance of concentric expansion chambers: an analytical, computational and experimental investigation.
5. A. Selamet, Z. L. Ji and P. M. Radavich 1998 *Journal of Sound and Vibration* **213**, 619–641. Acoustic attenuation performance of circular expansion chambers with offset inlet/outlet: II. Comparison with experimental and computational studies.
6. K. Hong and J. Kim 1995 *Journal of Sound and Vibration* **183**, 327–351. Natural mode analysis of hollow and annular elliptical cylindrical cavities.
7. A. Selamet and Z. L. Ji 1998 *Journal of Sound and Vibration* **214**, 580–587. Diametral plane-wave analysis for short circular chambers with end offset inlet/outlet and side extended inlet/outlet.
8. A. Selamet, N. S. Dickey and J. M. Novak 1994 *Journal of the Acoustical Society of America* **96**, 3177–3185. The Herschel–Quincke tube: a theoretical, computational, and experimental investigation.